Inhibition of NAD+-dependent histone deacetylases (sirtuins) causes growth arrest and activates both apoptosis and autophagy in the pathogenic protozoan *Trypanosoma cruzi*

PHERCYLES VEIGA-SANTOS[1,2], LISSA CATHERINE REIGNAULT[1,2], KILIAN HUBER[3,4], FRANZ BRACHER[3], WANDERLEY DE SOUZA[1,2,5] *and* TECIA MARIA ULISSES DE CARVALHO[1,2]*

[1] *Laboratório de Ultraestrutura Celular Hertha Meyer, CCS, Instituto de Biofísica Carlos Chagas Filho, Universidade Federal do Rio de Janeiro, Bloco G, Ilha do Fundão, Rio de Janeiro, CEP 21941-902, Brazil*
[2] *Instituto Nacional de Ciência e Tecnologia em Biologia Estrutural e Bioimagens, Universidade Federal do Rio de Janeiro, Cidade Universitária, Ilha do Fundão, Rio de Janeiro, Brazil*
[3] *Department of Pharmacy, Center for Drug Research, Ludwig-Maximilians-University of Munich, Butenandtstrasse 5-13, 81377 Munich, Germany*
[4] *CeMM Research Center for Molecular Medicine of the Austrian Academy of Sciences, Lazarettgasse 14, A-1090 Vienna, Austria*
[5] *Instituto Nacional de Metrologia, Qualidade e Tecnologia – Inmetro, Duque de Caxias, Rio de Janeiro, Brazil*

SUMMARY

Chagas disease, which is caused by the parasite *Trypanosoma cruzi*, affects approximately 7–8 million people in Latin America. The drugs available to treat this disease are ineffective against chronic phase disease and are associated with toxic side effects. Therefore, the development of new compounds that can kill *T. cruzi* at low concentrations is critically important. Herein, we report the effects of a novel 3-arylideneindolin-2-one that inhibits sirtuins, which are highly conserved proteins that are involved in a variety of physiological processes. The compound KH-TFMDI was tested against the epimastigote, trypomastigote and amastigote forms of *T. cruzi*, and its effects were evaluated using flow cytometry, light and electron microscopy. KH-TFMDI inhibited the replication of *T. cruzi* intracellular amastigotes with an IC_{50} of $0.5 \pm 0.2\,\mu M$, which is significantly lower than the IC_{50} of benznidazole. The compound also lysed the highly infectious bloodstream trypomastigotes (BST) with LC_{50} values of $0.8 \pm 0.3\,\mu M$ at $4\,°C$ and $2.5 \pm 1.1\,\mu M$ at $37\,°C$. KH-TFMDI inhibited cytokinesis and induced several morphological changes in the parasite, leading to its death by apoptosis and autophagy. This study highlights sirtuins as a potential new target for Chagas disease therapy.

Key words: Chagas disease, sirtuin inhibitors, KH-TFMDI, autophagy, apoptosis.

INTRODUCTION

Chagas disease is caused by *Trypanosoma cruzi* and affects approximately 7–8 million people in Latin America (WHO, 2013). The currently available chemotherapeutic agents for Chagas disease are nifurtimox and benznidazole, both of which are effective in the acute stage; however, their efficacy is very limited during the later chronic stage. In addition, both drugs demonstrate poor activity against many *T. cruzi* isolates and exhibit considerable side effects that can lead to the discontinuation of the therapy (Soeiro and Castro, 2011). In recent years, several studies have been carried out to identify selective and metabolic targets for Chagas disease therapy. Among these, sterol biosynthesis has been studied in some detail, and several inhibitors of this metabolic pathway are considered the most advanced candidate treatments, including posaconazole, which inhibits the sterol C14-demethylase of the protozoan (Urbina, 2010).

Class III histone deacetylases (HDACs), also known as sirtuins, are highly conserved from Archaea to higher eukaryotes. To date, seven different human sirtuins (SIRT1 to SIRT7) have been reported. SIRT1 is involved in cell calorie restriction, fat mobilization and the regulation of autophagic degradation and works together with SIRT3 to promote lifespan extension in various organisms (Salminen and Kaarniranta, 2009; Nakagawa and Guarente, 2011). SIRT2 is responsible for tubulin deacetylation, while SIRT3, SIRT4 and SIRT5 are associated with stress responses and mitochondrial metabolism. SIRT6 is involved in DNA repair

* Corresponding author: Laboratório de Ultraestrutura Celular Hertha Meyer, Instituto de Biofísica Carlos Chagas Filho, Universidade Federal do Rio de Janeiro, Centro de Ciências da Saúde, Bloco G, Cidade Universitária, Ilha do Fundão, Rio de Janeiro, CEP 21949-900, Brazil. E-mail: tecia@biof.ufrj.br
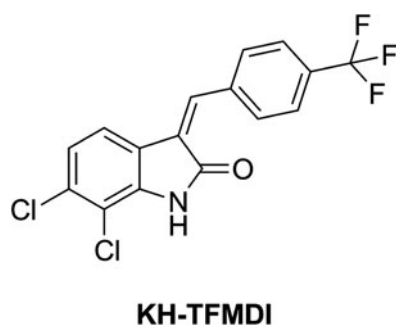
KH-TFMDI

Fig. 1. Chemical structure of KH-TFMDI.

mechanisms, and SIRT7 activates RNA polymerase (Nakagawa and Guarente, 2011). Several sirtuins have been identified in the genomes of various protozoa. Indeed, *T. cruzi* possesses two sirtuin-like genes, TcSIR2rp1 and TcSIR2rp3. However, the functions and localization of the products of these genes are currently unknown (Religa and Waters, 2012). In *Leishmania*, sirtuins are involved in the virulence and survival of the parasite and demonstrate differential distribution patterns during the cell cycle (Zemzoumi *et al.* 1998). In the bloodstream forms of *Trypanosoma brucei*, SIRT2 localizes to the nucleus and the mitochondria of the parasite and is involved in DNA repair (Alsford *et al.* 2007).

Recently, the sirtuin pathway has been studied extensively, and the results of these studies have indicated that sirtuin activator/inhibitor drugs have great potential in the treatment of several diseases, including those caused by protozoa (Baur *et al.* 2012; Zheng, 2013). Herein, we report the effects of the novel sirtuin inhibitor KH-TFMDI, a 3-arylideneindolin-2-one, based on a 6,7-dichloro-2-oxindole scaffold, which showed *in vitro* activity against mammalian SIRT1-3 (Huber *et al.* 2010). At very low concentrations, this compound was able to inhibit the replication of the epimastigote and amastigote forms. In addition, KH-TFDMI caused the lysis of the highly infective bloodstream trypomastigote forms. Microscopic analysis of treated parasites revealed significant morphological changes that led to the interruption of cell division and the activation of apoptosis and autophagy.

MATERIALS AND METHODS

Drug solutions

The sirtuin inhibitor KH-TFMDI (Fig. 1) was synthesized by Huber and Bracher (Huber *et al.* 2010) at the Department of Pharmacy, Center for Drug Research, Ludwig-Maximilians-University in Munich, Germany. A stock solution of the compound (10 mM) was prepared in dimethyl sulfoxide (DMSO) (Merck, Darmstadt, Germany), and the final concentration of DMSO in the experiments never exceeded 0·05%.

Parasites and host cell culture

All of the assays were performed using *T. cruzi* epimastigotes, trypomastigotes and intracellular amastigotes of the Y strain (TcII) (Zingales *et al.* 2009). Trypomastigotes were obtained from the supernatants of previously infected LLC-MK$_2$ cells at 7 days post-infection. Bloodstream trypomastigotes (BST) were obtained from infected Swiss CF1 mice at the peak of parasitaemia by differential centrifugation (Meirelles *et al.* 1982). Epimastigotes were cultivated in LIT medium supplemented with 10% fetal bovine serum (FBS) (GIBCO, Grand Island, NY) (Camargo, 1964). Resident peritoneal macrophages were obtained from Swiss CF1 mice and cultivated in RPMI medium (GIBCO, Grand Island, NY) supplemented with 10% FBS at 37 °C in a 5% CO_2 atmosphere.

Cytotoxicity in peritoneal macrophages

Peritoneal macrophages were obtained as previously described and cultured for 24 h. Thereafter, the cells were treated with KH-TFMDI (10–100 μM) and incubated for 96 h at 37 °C. Fresh RPMI-1640 medium containing only 10% FBS was added to untreated samples (control). To analyse the toxicity effects, the MTS/PMS (3-(4,5-dimethyl-2-thiazolyl)-5-(3-carboxymethoxy-phenyl)-2-(4-sulfophenyl)-2H-tetrazolium inner salt/5-methylphenazinium methyl sulfate) assay was performed as described by Henriques *et al.* (2011). The selectivity index of KH-TFMDI was also determined based on its activity against the trypomastigote and intracellular amastigote forms of *T. cruzi*, as follows: (ratio: 50% cytotoxic concentration [CC_{50}] mammalian cells/ half maximal inhibitory concentration [IC_{50}] protozoans). All experiments were performed in duplicate. The means were determined based on at least three experiments.

Antitrypanosomal activity

For the antiproliferative assay involving the epimastigote forms, 1×10^6 parasites mL^{-1} were cultivated in LIT medium supplemented with 10% FBS. After 24 h of epimastigote growth, concentrations of 5 to 80 μM of KH TFMDI were added to the culture and incubated for 96 h at 28 °C. Cells were collected every 24 h for cell counting in a Neubauer chamber. Two controls consisted of LIT supplemented with 10% FBS and LIT + 0·05% DMSO. Then, the cells were allowed to adhere to the coverslips with 0·1 mg mL^{-1} poly-L-Lysine, fixed with Bouin's solution and stained with Giemsa for morphological analysis under a Zeiss Axioplan 2 light microscope (Oberkochen, Germany) equipped with a Color View XS digital video camera.

To investigate the effect of KH-TFMDI on the amastigote form, peritoneal macrophages were

seeded as previously described and incubated with *T. cruzi* BST at a ratio of 10 parasites to 1 macrophage for 2 h. Non-internalized parasites were removed by washing, and the host cells were incubated for 24 h at 37 °C to allow the full internalization and differentiation of trypomastigotes to amastigotes. Fresh 10% FBS–RPMI-1640 medium alone (control) or containing KH-TFMDI ($0\cdot5$–$10\,\mu$M) was added to infected cells, and the cells were incubated for 96 h at 37 °C. Infected cultures were fixed in Bouin's solution and stained with Giemsa. Parasite infection was quantified under a Zeiss Axioplan light microscope (Jena, Germany) equipped with a $100\times$ lens. The antiproliferative assay was performed as described by Veiga-Santos *et al.* (2012). Infection indexes (i.e. the percentage of infected host cells multiplied by the average number of intracellular amastigotes per infected host cell) were determined by counting a total of 500 host cells and then used as a parameter to calculate the intensity of infection under each condition tested in the study. Drug activity was calculated using the SigmaPlot® (version 10) program (Systat Software Inc., San Jose, CA, USA). The results are expressed as the mean of three independent experiments.

For bloodstream trypomastigote assays, 5×10^{6} parasites mL^{-1} were incubated for 24 h at 4 and 37 °C in RPMI-1640 medium supplemented with 90% mouse blood in the presence or absence of KH-TFMDI at concentrations ranging from 1 to $5\,\mu$M (Silva *et al.* 2011). This experiment was also performed with trypomastigotes obtained from the supernatant of a previously infected cell line LLC-MK$_2$. Between 5 to 7 days after infection protozoa were collected from the supernatants of infected LLC-MK$_2$ cells and incubated with fresh RPMI-1640 medium supplemented with 0·5% FBS, with or without KH-TFMDI ($0\cdot1$ to $5\,\mu$M), for 24 h at 37 °C under a 5% CO$_2$ atmosphere. The concentration of KH-TFMDI at which 50% of the parasites were lysed (LC$_{50}$) was calculated by counting the cells in a Neubauer chamber. The experiment was performed in duplicate for each of the three different experiments.

To compare the control and treated groups in all assays, paired *t*-tests and a 95% confidence interval were applied (GraphPad Prism v.5.00 for Windows; GraphPad Software Inc., San Diego, CA).

Flow cytometry

For flow cytometry assays, epimastigotes were treated with 7 and $10\,\mu$M of KH-TFMDI and incubated for 96 h at 28 °C. In addition, the trypomastigotes obtained from the supernatants of previously infected LLC-MK$_2$ cells were treated with $1\cdot8\,\mu$M TFMDI and incubated for 24 h. After treatment, the parasites were washed, suspended in annexin V binding buffer and incubated at room temperature for 15 min with annexin V – Alexa 488 (Dead Cell Apoptosis Kit with Annexin V Alexa Fluor® 488 & PI; Molecular Probes®). Propidium iodide from the same kit was added to the samples at the moment of acquisition. Data were collected on a BD FACSCalibur® instrument controlled by CellQuest Pro® software (BD Biosciences, San Jose, CA, USA) and analysed with Summit 4.3® (Dako Colorado, Inc., Fort Collins, CO, USA). Ten thousand gated events were analysed in each sample. The values were organized in column graphs, and statistical analysis was performed using Student's *t*-test. The values are presented as the mean $\pm$ S.E.M. The results were considered to be significant when $P<0\cdot05$.

Scanning electron microscopy (SEM)

Trypanosoma cruzi epimastigotes were incubated with KH-TFMDI ($7\,\mu$M) for 96 h at 28 °C. Trypomastigotes obtained from LLC-MK$_2$ cells were incubated with $1\cdot8\,\mu$M of the drug for 24 h at 37 °C. Subsequently, the samples were fixed in 2·5% glutaraldehyde in 0·1 M phosphate buffer (pH 7·2), processed for SEM as previously described (Veiga-Santos *et al.* 2012) and observed under a Quanta X50 Scanning Electron Microscope. Images were obtained and processed using XTm version 4.1.1.1935 (FEI Company).

Transmission electron microscopy (TEM)

For TEM, epimastigotes were treated with KH-TFMDI ($7\,\mu$M) and incubated for 120 h. Trypomastigotes were incubated with $1\cdot8\,\mu$M of the drug for 24 h. Macrophages were infected for 24 h and subsequently treated with $1\,\mu$M of KH-TFMDI for 96 h. After the experimental procedure, the samples were fixed and processed as previously described (Macedo-Silva *et al.* 2011). The samples were observed under a JEOL JEM-1200EX transmission electron microscope operating at 80 kV.

Fluorescence microscopy

For the fluorescence assays, epimastigotes were treated with $10\,\mu$M KH-TFMDI and incubated for 96 h at 28 °C; macrophages were infected for 24 h and then treated with $1\,\mu$M of KH-TFMDI for 96 h. The samples were fixed in 4% formaldehyde, permeabilized with 0·1% saponin in 3% bovine serum albumin (BSA) in PBS (pH 8·0) for 30 min at room temperature and washed with the BSA solution with saponin for 15 min. For the autophagy assays, cells were incubated overnight with a 1:100 dilution of rabbit anti-LC3B antibody (Sigma). To evaluate tubulin localization, cells were incubated for 2 h with a 1:200 dilution of mouse anti-α tubulin antibodies. Then, the samples were incubated with 1:400 Alexa
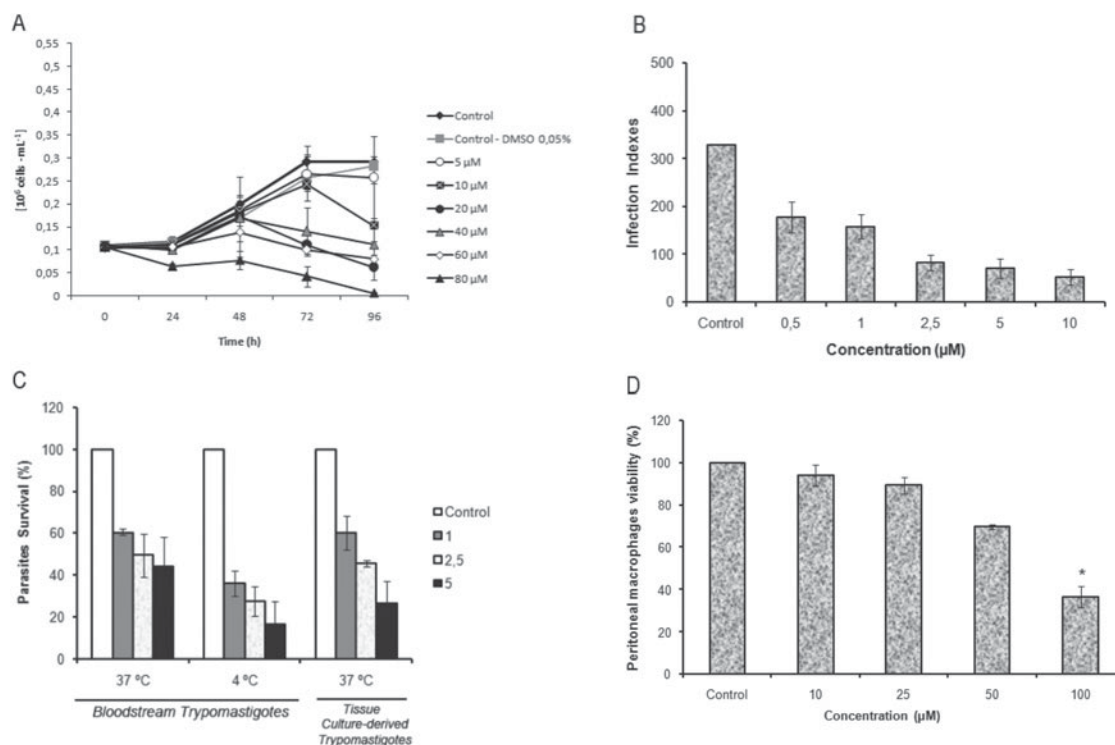
Fig. 2. (A) Growth of the *T. cruzi* epimastigotes (Y strain, TcII) treated with KH-TFMDI for 96 h at 28 °C. The parasite was cultured in the absence (control) or presence of KH-TFMDI at concentrations from 5 to 80 μM. (B) The effect of KH-TFMDI on intracellular amastigotes. Peritoneal macrophages were infected with trypomastigotes for 2 h and then washed and incubated with complete medium for 24 h. Then, the infected cells were treated with 0·5–10 μM KH-TFMDI for 96 h. The infection indexes were calculated using these results. All results were significant at $P < 0.0001$. (C) The effects of KH-TFMDI on *T. cruzi* isolated from the bloodstream and on tissue culture-derived trypomastigotes. The activity was evaluated after 24 h of treatment at 4 or 37 °C. All results were significant at $P < 0.05$. (D) The effect of KH-TFMDI on peritoneal macrophage viability. Peritoneal macrophages were cultured for 24 h and then incubated with the compound (at concentrations ranging from 10–100 μM) for 96 h at 37 °C under 5% CO_2. Then, peritoneal macrophages were incubated with MTS/PMS at 37 °C for 2 to 4 h, and the absorbance read at 490 nm in a microplate reader. (*) indicates significance at $P < 0.05$. The bar represents the standard deviation. All experiments were performed in triplicate, and each set of experiments was repeated at least three times.

Fluor 546 (red)-labelled or 1:100 Alexa Fluor 488 (green)-labelled secondary antibodies at room temperature for 1 h (Molecular Probes). After rinsing in PBS (pH 8·0) containing 3% BSA, the coverslips were incubated with Hoechst dye for DNA staining (Molecular Probes). The cells were observed under a Zeiss Axioplan microscope. As a positive control for the induction of autophagy, the epimastigotes were treated with 0·05 mg mL^{-1} rapamycin for 2 h prior to the experiment.

Ethical guidelines

This study was approved by the Ethics Committee of the Carlos Chagas Filho Biophysics Institute in the Health Sciences Center of Rio de Janeiro Federal University (Licence number: IBCCF106). All animals received humane care in compliance with the Principles of Laboratory Animal Care of the National Society for Medical Research and the Guide for the Care and Use of Laboratory Animals prepared by the USA National Institutes of Health.

RESULTS

Inhibition of cell growth and the induction of trypomastigote lysis

The sirtuin inhibitor KH-TFMDI (Fig. 1) was tested against all forms of *T. cruzi*. The compound exhibited a dose-dependent inhibitory effect on parasite growth with IC$_{50}$ values of 7 ± 0.51 and 0.5 ± 0.2 μM for the epimastigote and amastigote forms, respectively (Fig. 2A and B). The IC$_{50}$ of the reference drug benznidazole, which is presently used to treat Chagas disease, was 8 ± 0.3 and 2.8 ± 0.3 μM, respectively. A drastic reduction in both the percentage of infected macrophages and the mean number of intracellular amastigotes per cell was also observed. All of these results were significantly different from those of the control group at $P \leqslant 0.05$ according to Student's *t*-test.

Table 1. *Morphological alterations caused by KH-TFMDI treatment in T. cruzi epimastigotes after 96 h of incubation at 28 °C*

Alteration	Control (%)[a]	7 μM KH-TFMDI (%)[a]
Kinetoplast rounding	$4 \cdot 4 \pm 3 \cdot 11$	$45 \pm 6 \cdot 06$
Flagellum detachment	0	$70 \pm 10 \cdot 21$
Cytokinesis inhibition	0	$37 \pm 8 \cdot 56$
Cell body rounding	$2 \cdot 5 \pm 0 \cdot 7$	$26 \pm 12 \cdot 26$

[a] A total of 500 cells were evaluated in each group.

KH-TFMDI showed a strong lytic activity against tissue culture-derived trypomastigotes (TCT) and BST; indeed, approximately 50% of TCT were killed at a concentration of $1 \cdot 6 \pm 0 \cdot 18 \, \mu$M at 37 °C. Against BSTs, an LC_{50} of $0 \cdot 8 \pm 0 \cdot 3 \, \mu$M at 4 °C was observed. For comparison, crystal violet, the drug that is currently routinely used in blood banks to control infection by blood transfusion, has an LC_{50} of $11 \cdot 5 \, \mu$M. When the incubation was carried out at 37 °C, KH-TFMDI showed an LC_{50} of $2 \cdot 5 \pm 1 \cdot 1 \, \mu$M (Fig. 2C), while benznidazole showed an LC_{50} greater than $400 \, \mu$M against BSTs at 37 °C (data not shown).

Effects on host cells

The effects of KH-TFMDI on mammalian cells were evaluated in peritoneal macrophages after 96 h of incubation at 37 °C via the MTS/PMS assay (Henriques *et al.* 2011). The 50% cytotoxic effects (CC_{50}) value of KH-TFMDI in the macrophages was $81 \pm 12 \, \mu$M (Fig. 2D).

Effects on parasite structure

Epimastigotes that were incubated with $7 \, \mu$M KH-TFMDI exhibited several changes that could be observed using light microscopy. KH-TFMDI treatment for 96 h altered the kinetoplast shape in 45% of the parasites, interfered with the process of cytokinesis in approximately 37% of cells, and caused rounding of the parasite body in approximately 26% of the parasites. In addition, KH-TFMDI caused the detachment of the flagellum from the cell body in approximately 70% of the epimastigotes (Table 1). To better visualize this flagellum detachment, epimastigotes treated with $7 \, \mu$M KH-TFMDI for 120 h were analysed by fluorescence microscopy using an anti-α tubulin antibody and Hoechst stain to label the nucleus (Fig. 3).

We also used SEM and TEM to analyse the effects of KH-TFMDI on the protozoan structure. Untreated *T. cruzi* epimastigotes exhibited a typical elongated shape with a smooth cell surface (Supplementary Figure S1A). In contrast, parasites treated with $7 \, \mu$M KH-TFMDI for 96 h revealed severe morphological changes in the parasite body, such as the detachment of the parasite flagellum and an inhibition of cytokinesis leading to the failed separation of the newly formed protozoans. We also observed a depression and disruption of the plasma membrane and an intense wrinkling of the parasite surface (Figure S1 B–D).

Figure 4A shows a section of an untreated epimastigote highlighting different organelles, such as the mitochondrion, nucleus, kinetoplast and flagellum, with normal ultrastructure. Epimastigotes treated with $7 \, \mu$M KH-TFMDI for 12 h (Fig. 4B) and 24 h (Fig. 4C and D) showed a progressive loss of kDNA compaction. In addition, the drug also induced other morphological changes, varying from discrete alterations to a total destruction of the parasite, depending on the time of drug incubation. After 48 to 96 h of incubation, we observed four main points of cell alterations: an increase in the number of lipid-storage bodies, an accumulation of medial cisternae of the Golgi complex, large structures resembling myelin-like figures localized near the flagellum, and the appearance of unpacked nuclear chromatin (Fig. 4E and G–I). In addition, well-developed endoplasmic reticulum (ER) profiles were observed surrounding reservosomes and lipid-storage bodies after 72 h of treatment (Fig. 4G and H).

The treatment of intracellular amastigote forms with KH-TFMDI also caused alterations in the parasite plasma membrane, such as a loss of cytoplasmic contents, disruption of the plasma membrane, membrane shedding, nuclear membrane detachment and membrane convolutions, thereby completely altering the parasite morphology (Fig. 5B–F).

Trypomastigotes treated with $1 \cdot 8 \, \mu$M KH-TFMDI for 24 h revealed alterations similar to those observed in epimastigotes (Supplementary Fig. S2). Note that untreated trypomastigotes exhibited characteristic morphology, as evidenced by SEM (Fig. S2A), and TEM revealed that the organelles, including the mitochondrion, nucleus, kinetoplast and flagellum, were also normal (Fig. S2D). KH-TFMDI caused disorganization of the parasite plasma membrane, with bleb formation and intense wrinkling of the cell surface (Fig. S2B and C). The drug also altered nuclear chromatin and kDNA compaction (Fig. S2E). Lipid body accumulation was also observed in the trypomastigote forms (Fig. S2F).

The mechanism of killing of the parasite

Two types of observed morphological changes provide some insight into the mechanism of parasite death induced by KH-TFMDI. After incubation for 12 or 24 h, the unpacking of nuclear chromatin, which is indicative of apoptosis, was observed (Fig. 4C and D). After 24 h of treatment with $10 \, \mu$M KH-TFMDI, approximately 92% of the epimastigotes
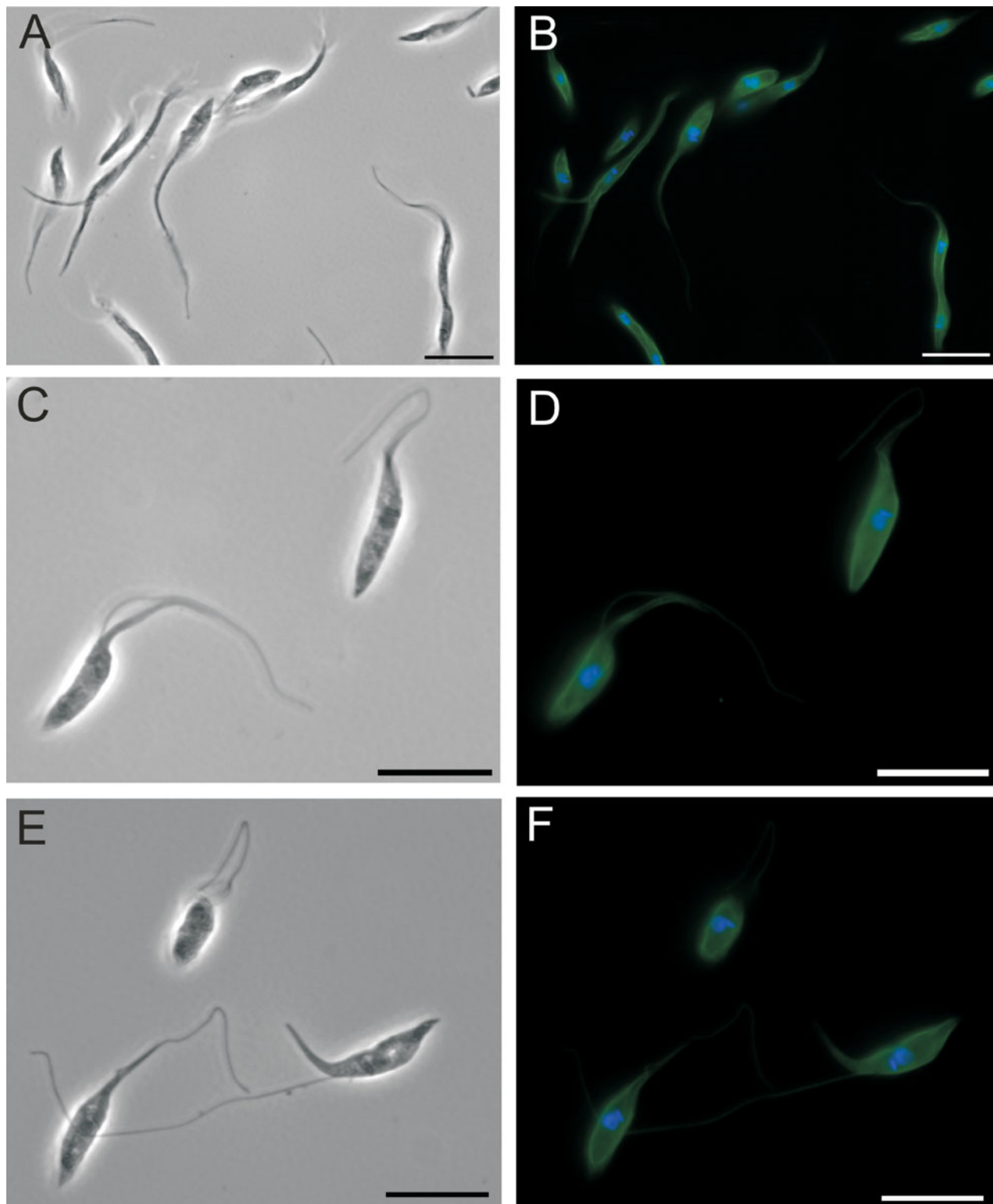
Fig. 3. Immunofluorescence microscopy demonstrating flagellum detachment in treated epimastigotes (7 μM KH-TFMDI for 120 h). The cells were labelled with anti-α-tubulin for 2 h and with an Alexa Fluor 488 (green)-labelled secondary antibody for 1 h. Hoechst stain (5 μg mL^{-1}) was used to label the DNA (blue). (A, B) In untreated epimastigotes, the flagellum is attached to the parasite body; (C–F) in epimastigotes treated with KH-TFMDI, the flagellum is detached from the parasite body; (A, C, E) phase contrast images; (B, D, F) merged images of Hoechst and α-tubulin labelling. Bars: 10 μm.

were labelled with annexin V (Fig. 6A), which binds to phosphatidylserine (PS), a phospholipid related to apoptotic events (Lee *et al*. 2013). However, no disruption of the plasma membrane was observed;

the percentage of propidium iodide (PI)-positive cells was lower than 1% (data not shown). After 48 and 72 h of treatment, we observed a similar labelling pattern, with 87 and 88% of treated parasites positive
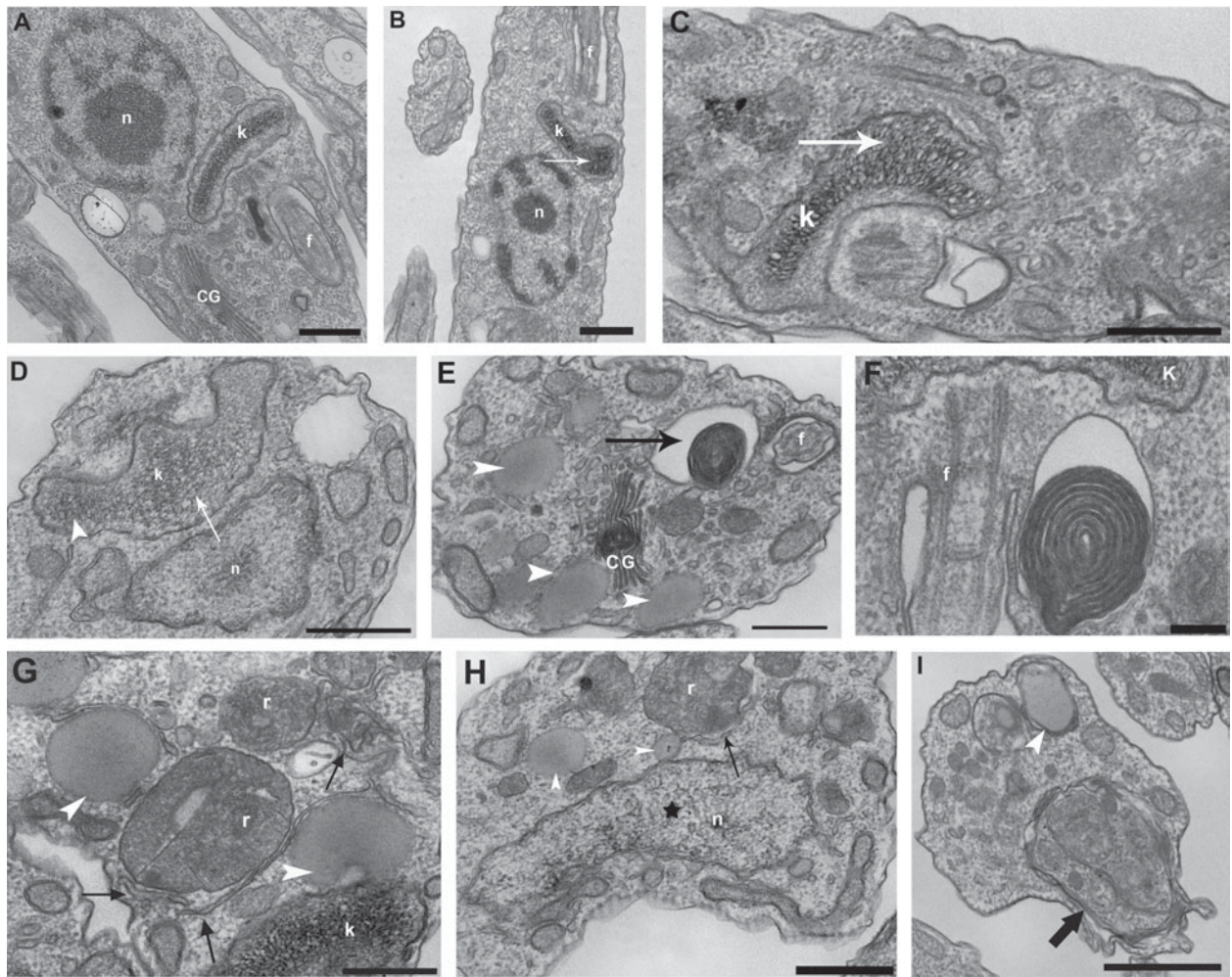
Fig. 4. TEM images of *T. cruzi* epimastigotes treated with 7 or $10\,\mu$M KH-TFMDI. (A) Untreated epimastigotes exhibit organelles with normal morphology. Kinetoplast (k), nucleus (n), Golgi (CG) and flagellum (f) after 96 h of incubation. Epimastigotes treated with $7\,\mu$M for 12 h (B) and 24 h (C, D) show an aberrant loss of kDNA compaction inside the mitochondrion (white arrow and arrowhead); (E, F) epimastigotes treated for 48 and 72 h contain large structures similar to myelin-like figures (black arrow). After 48 to 96 h of treatment, lipid-storage bodies (white arrowhead) (E–I) and the accumulation of cisternae in the medial region of the Golgi complex were observed (only in E); (G, H) in epimastigotes after 72 h of treatment, well-developed endoplasmic reticulum membranes surrounding reservosomes, lipid-storage bodies (arrow) and abnormal nucleus condensation (star) were observed; (I) after 120 h of treatment, autophagosome formation (large black arrow) and membranes surrounding the lipid-storage body (white arrowhead) were observed. Bar: (A–D) $0\cdot5\,\mu$m; (E, F) $2\,\mu$m; (G, H) $5\,\mu$m; (I) $1\,\mu$m.

for annexin V (Fig. 6A), and the proportion of PI-positive parasites increased to almost 2 and 4% (data not shown). However, after 96 h of treatment, we observed a significant reduction in PS-positive epimastigotes, such that only 50% of cells were PS positive (Fig. 6A). In the case of trypomastigotes, after 24 h of treatment with $1\cdot8\,\mu$M KH-TFMDI, we observed that 40% of parasites were positive for Annexin V (Fig. 6B), and half of these parasites (20%) were already positive for PI, indicating that apoptosis had occurred. However, only 3% of trypomastigotes were positive only for PI, and less than 1% of untreated trypomastigotes were positive for PI (data not shown). Unfortunately, all attempts to carry out similar experiments with intracellular amastigotes were unsuccessful (data not shown).

Analyses of epimastigotes treated for 72 and 96 h revealed the presence of ER profiles surrounding structures such as the reservosomes and lipid-storage bodies (Fig. 4G and H). The obtained images are indicative of autophagy. Autophagy was confirmed by labelling the drug-treated epimastigotes with an anti-LC3B antibody (i.e. to label microtubule-associated protein light chain 3) that is widely employed to identify autophagic structures by fluorescence microscopy (Fig. 7). Strong labelling of the structures was observed in treated parasites (Fig. 7F), whereas no labelling was observed in untreated epimastigotes (Fig. 7C). Rapamycin, a drug that induces autophagy, was used as a positive control at a concentration of $0\cdot05\,\mu$g mL^{-1} (Fig. 7I), demonstrating the functionality of the assay. We also
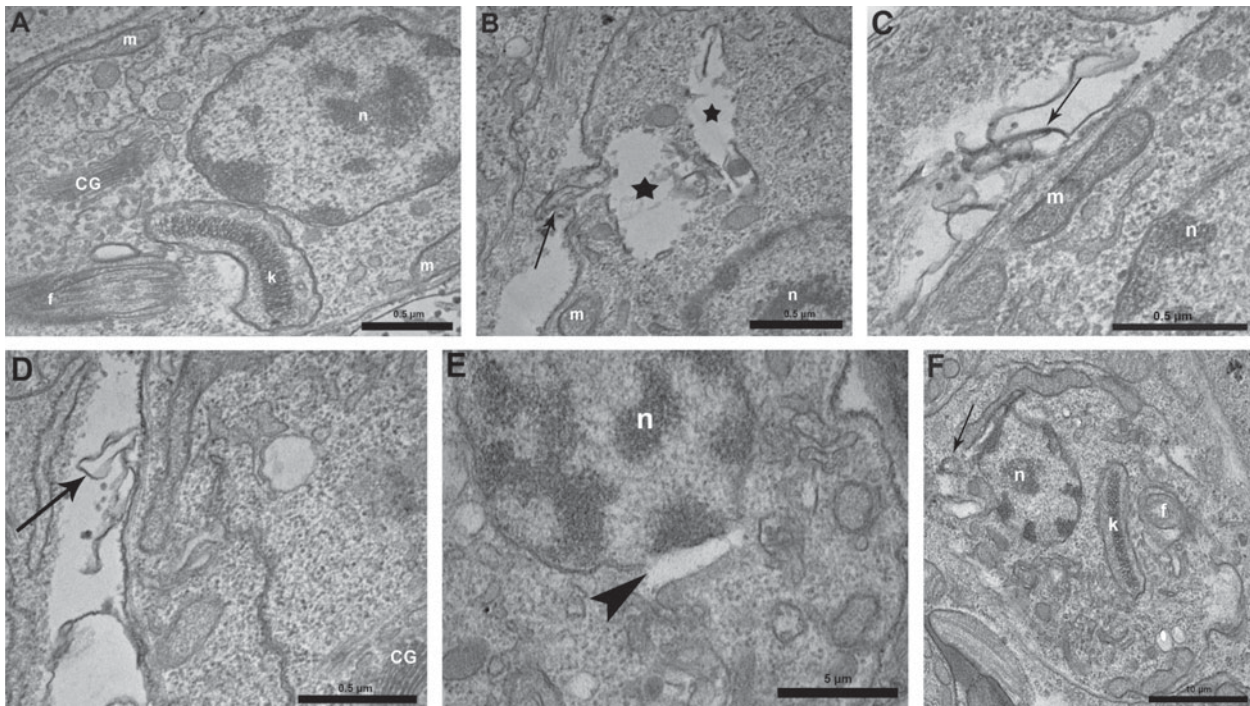
Fig. 5. TEM images of *T. cruzi* intracellular amastigotes treated with 1 μM KH-TFMDI for 96 h. (A) Untreated intracellular amastigote: kinetoplast (k), mitochondrion (m), nucleus (n), Golgi (CG) and flagellum (f); (B) treatment caused plasma membrane disruption (arrow) and a loss of cytoplasmic content (stars); (C, D) plasma membrane shedding (arrow); (E) nuclear membrane detachment (arrowhead); and (F) severe alterations in the plasma membrane, leading to convolutions and the loss of parasite plasma membrane integrity (arrow).
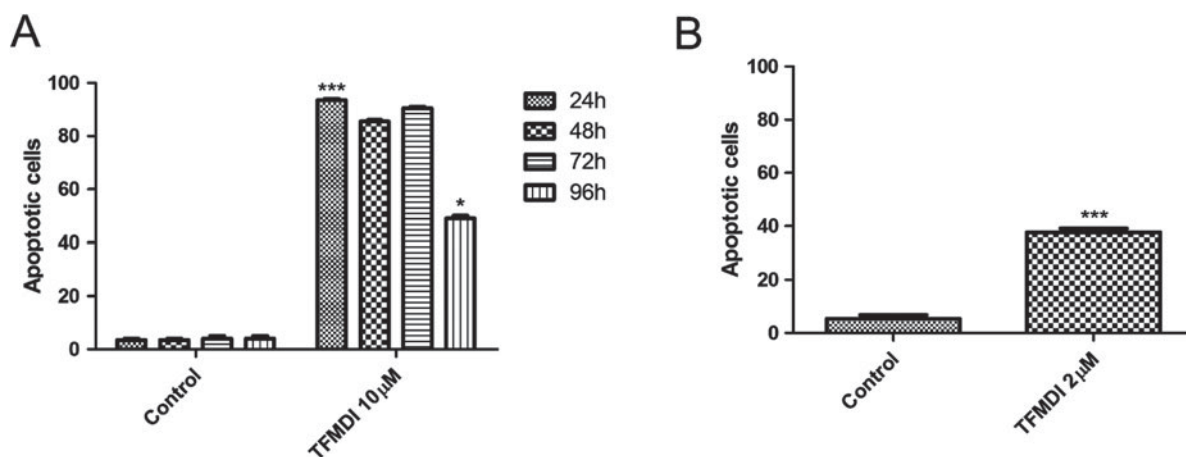

Fig. 6. Column graphs representing flow cytometry experiments on *T. cruzi* epimastigotes (A) and trypomastigotes (B). Epimastigotes were treated with 10 μM of KH-TFMDI for 24, 48, 72 or 96 h, while trypomastigotes were treated with 1·8 μM KH-TFMDI for 24 h. After incubation, treated or control parasites were washed, resuspended in Annexin V Binding Buffer, incubated with Annexin V/PI and analysed on a BD FACSCalibur®, as described in the Materials and Methods section. (A) After 24 h of treatment, 92% of epimastigotes were positive for Annexin V. After 96 h of treatment, only 40% of epimastigotes presented the same labelling pattern. (B) After 24 h of treatment, 40% of trypomastigotes were already positive for Annexin V. Ten thousand gated events were counted from each sample. The statistical analysis was carried out using Student's *t*-test. Values are presented as the mean ± s.e.m. (***) $P < 0.0001$ (A and B) and (*) $P < 0.05$ (A).

analysed the activation of autophagy in treated intracellular amastigotes. Strong labelling of cytoplasmatic structures was observed in parasites treated with KH-TFMDI for 96 h (Fig. 8D). No LC3B labelling was observed in untreated amastigotes (Fig. 8B).

DISCUSSION

The observations reported here clearly show that the sirtuin inhibitor KH-TFMDI significantly interfered with all developmental stages of *T. cruzi*. Sirtuins in mammalian cells are associated with histone deacetylation, causing heterochromatin
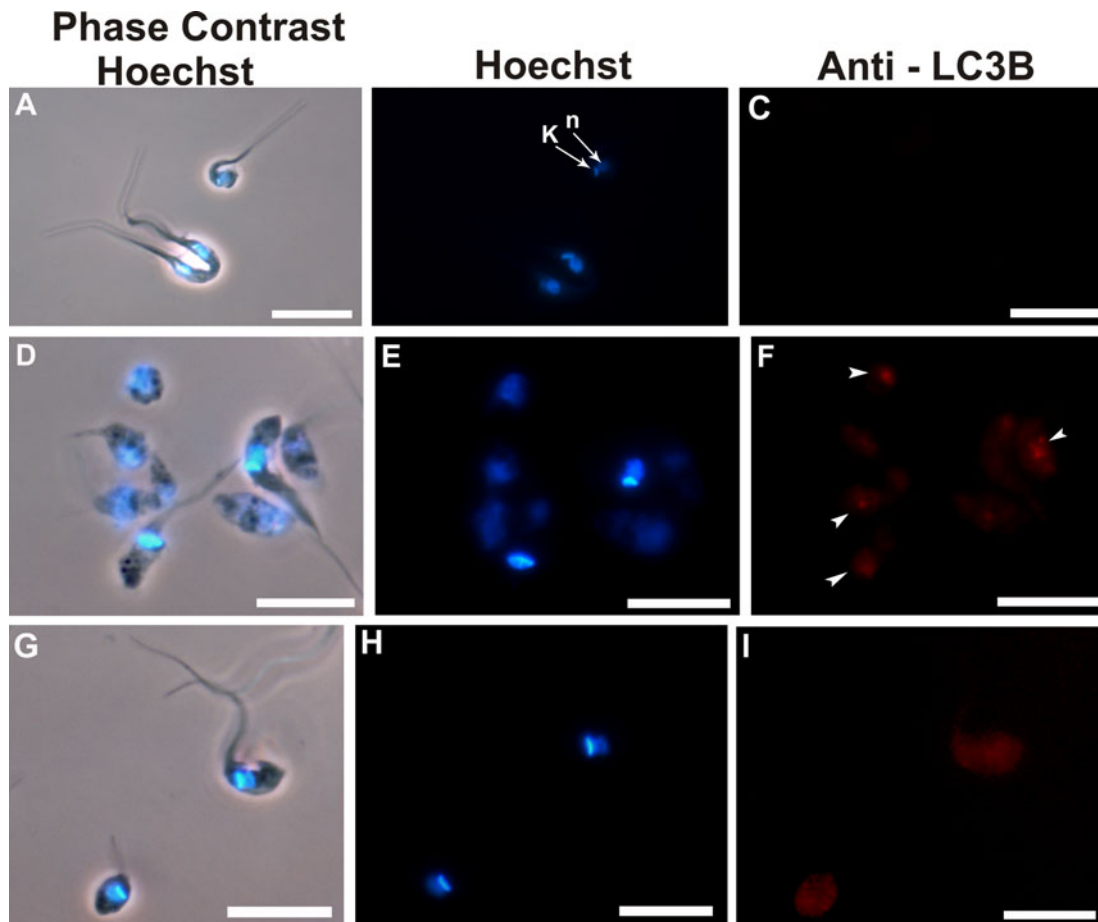
Fig. 7. Immunofluorescence microscopy demonstrating LCB3 labelling (i.e. a marker of autophagic cell death) of epimastigotes treated with $10\,\mu$M of KH-TFMDI. (A, C) Untreated epimastigotes after 96 h of incubation show only Hoechst labelling; epimastigotes treated with KH-TFMDI (D–F) and rapamycin (0.05 mg mL^{-1}) (G–I) exhibit intense red labelling (arrowhead). Bar: $5\,\mu$m.

formation and transcription repression (Nakagawa and Guarente, 2011). As previously discussed, *T. cruzi* encodes two sirtuin-like genes, TcSIR2rp1 and TcSIR2rp3, but the localization and function of the encoded proteins remain unclear (Religa and Waters, 2012).

At very low concentrations, the sirtuin inhibitor KH-TFMDI was able to inhibit the replication of the epimastigote forms, which proliferate in axenic cultures, and the amastigote form, which replicates in the cytoplasm of host cells and is responsible for the amplification of the infection. Interestingly, KH-TFMDI showed better activity against intracellular amastigotes than the reference drug benznidazole. In addition, KH-TFDMI caused the lysis of the highly infective bloodstream trypomastigote form and was more active than crystal violet. Moreover, treatment with crystal violet changes the colour of the blood to violet, which is not well accepted by some patients. These observations have encouraged us to initiate further studies focusing on the use of KH-TFMDI in blood banks.

One important criterion for potential anti-trypanosomal drugs is a low toxicity against mammalian cells. Here, KH-TFMDI was found to have significant selectivity indexes; it was 50-fold more selective against TCT and 162-fold more selective against intracellular amastigotes than peritoneal macrophages. Therefore, KH-TFMDI shows promising mammalian cell tolerance indexes compared with other drugs currently being used in clinical therapy. The reference drug benznidazole, which is used to treat Chagas disease, presents a CC_{50} value of $1218\,\mu$M in LLC-MK$_2$ cells (Cogo *et al*. 2012). However, this drug still has considerable side effects for patients, including hypersensitivity reactions, bone marrow depletion and peripheral polyneuropathy (Soeiro and Castro, 2011).

Recently, several molecules with the ability to inhibit/activate the deacetylase activity of sirtuins have shown anticancer, anti-HIV, anti-protozoan, metabolic and neurological activities (Baur *et al*. 2012; Zheng, 2013). Significant activities were found in assays testing this group of drugs against trypanosomatids. Bisnaphthalimidopropyl (BNIP), an anti-cancer drug, also showed strong and selective effects against the SIRT1 of *Leishmania infantum* (Tavares *et al*. 2010). In addition, suramin, a selective SIRT1 inhibitor with anti-proliferative effects, has been used to treat African trypanosomiasis since the
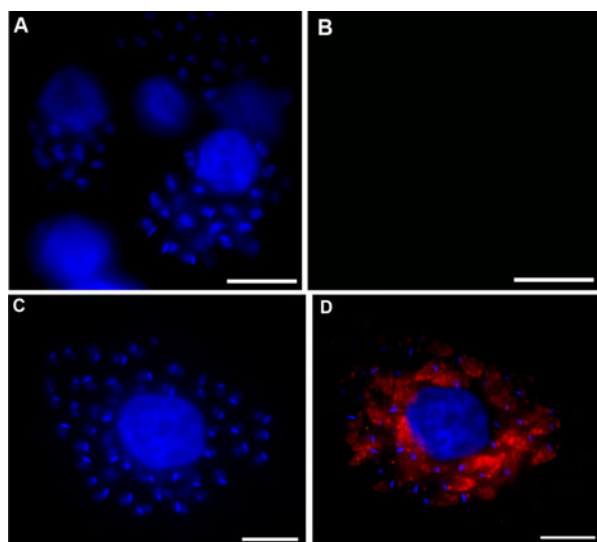
Fig. 8. Immunofluorescence microscopy of intracellular amastigotes labelled with antibodies against LC3B (microtubule-associated protein light chain 3), a marker of autophagic cell death (red), and Hoechst, a nuclear marker (blue). (A, B) Untreated infected macrophages after 96 h: (A) Hoechst labelling; (B) no anti-LC3B labelling was observed; (C, D) Intracellular amastigotes treated with 1 μM KH-TFMDI: (C) Hoechst labelling, (D) merge of Hoechst and anti-LC3B staining. Bars = 10 μm.

1920s and has also demonstrated activity against *T. cruzi*. The compound caused morphological changes in the amastigote and trypomastigote forms, interfering with cell division and differentiation processes. In addition, trypomastigotes obtained from suramin-treated host cells were significantly less infective than untreated parasites, and the amastigotes derived from those trypomastigote forms were less proliferative (Voogd *et al.* 1993; Bisaggio *et al.* 2008). Similar antiproliferative activities were also demonstrated for the compound sirtinol, a commercial SIRT2 inhibitor. This drug also blocked *L. infantum* amastigote multiplication and promoted cell death associated with DNA fragmentation (Vergnes *et al.* 2002, 2005).

As observed using light microscopy and SEM, KH-TFMDI inhibited cytokinesis and caused the detachment of the parasite flagellum. The flagellum is normally strongly attached to the cell body of *T. cruzi*. Studies have suggested that the flagellum-cell body attachment zone, known as FAZ, plays an important role in the establishment of the protozoan shape and in cell division by acting as a molecular organizing centre (Kohl and Bastin, 2003). The FAZ region also has another important function, i.e. indicating the precise site of cell division initiation. In cells with altered FAZ, cell separation is slowed or completely inhibited (Kohl *et al.* 2003). We observed that the separation of newly formed epimastigotes is blocked in KH-TFMDI-treated cells.

Treatment with KH-TFMDI also induced torsion and the rounding and thinning of the cell body in *T. cruzi*. These alterations may be indicative of the destabilization of cytoskeleton components or microtubule-associated proteins. Taxol, an anti-microtubule agent with activity against *T. cruzi*, also demonstrated intense morphological alterations of the parasite body that were similar to those induced by KH-TFMDI treatment (Dantas *et al.* 2003). Note that SIRT2 is a tubulin deacetylase that has the ability to control the level of tubulin acetylation, which affects the microtubule network (Nakagawa and Guarente, 2011).

The activation of autophagy, apoptosis, or both has previously been described in *T. cruzi*. Autophagy is a process in which cellular components, such as the cytoplasm, organelles and protein aggregates, are catabolized through the formation of structures with double membranes, known as autophagosomes. This process can cause cell death due to the extensive degradation of cell components or the non-selective degradation of important structures and organelles (Gump and Thorburn, 2011).

Because TEM findings revealed morphological alterations of the nuclear and mitochondrial DNA of the treated parasites, flow cytometry studies were conducted to explore whether KH-TFMDI could trigger programmed cell death in the epimastigote, trypomastigote and amastigote forms. Flow cytometry showed that treated epimastigotes and trypomastigotes were both positive for Annexin V, an early hallmark of apoptosis-like cell death (Lee *et al.* 2013). After 24, 48 and 72 h of treatment, 92, 87 and 88% of epimastigotes were positive for Annexin V, respectively. However, after 96 h of treatment, we observed a significant reduction in the proportion of PS-positive epimastigotes; only 50% of cells were PS positive at this time point. This significant reduction is due to the parasite death caused by severe morphological changes in the parasite body. In addition to the depression and disruption of the plasma membrane, the drug affects the microtubule network through events related to the capacity of sirtuins to control tubulin acetylation (Nakagawa and Guarente, 2011). In the case of the trypomastigotes, 20% of parasites were positive for annexin V, 20% were double positive for annexin V and PI, and only 3% of trypomastigotes were positive for PI only. These data suggest that apoptosis is the first cell death event that takes place when epimastigotes and trypomastigotes are treated with KH-TFMDI.

As reviewed by Verdin *et al.* (2010), sirtuin inhibitors interfere directly with mitochondrial metabolism, including energy production, signalling events and even apoptosis. Nevertheless, the drug also induced the activation of autophagic mechanisms in epimastigotes and intracellular amastigotes. In a recent study using a triazolic naphthofuranquinone, Fernandes *et al.* (2012) also observed the presence

of endoplasmic ER surrounding reservosomes. These authors also suggested that the presence of this membrane network is associated with an increase in monodansylcadaverine labelling, which is an indicator of autophagy activation. We confirmed the activation of autophagy by immunofluorescence microscopy.

In conclusion, our results suggest that KH-TFMDI impairs epimastigote and amastigote proliferation by causing drastic alterations in the ultrastructure of *T. cruzi* and induces the activation of apoptosis and autophagy mechanisms that lead to cell death. In addition, KH-TFMDI also showed important trypanosomicidal activity against BTs. Collectively, the results of the present study indicate that sirtuin inhibitors are potential new compounds for the treatment of Chagas disease and blood control in blood banks.

REFERENCES

Alsford, S., Kawahara, T., Isamah, C. and Horn, D. (2007). A sirtuin in the African trypanosome is involved in both DNA repair and telomeric gene silencing but is not required for antigenic variation. *Molecular Microbiology* **63**, 724–736. doi: 10.1111/j.1365-2958.2006.05553.x.

Baur, J. A., Ungvari, Z., Minor, R. K., Le Couteur, D. G. and Cabo, R. (2012). Are sirtuins viable targets for improving healthspan and lifespan? *Nature Review Drug Discovery* **11**, 443–461. doi: 10.1038/nrd3738.

Bisaggio, D. F. R., Adade, C. M. and Souto-Padrón, T. (2008). *In vitro* effects of suramin on *Trypanosoma cruzi*. *International Journal of Antimicrobial Agents* **31**, 282–286. doi: 10.1016/j.ijantimicag.2007.11.001.

Camargo, E. P. (1964). Growth and differentiation in *Trypanosoma cruzi*. Origin of metacyclic trypanosomes in liquid media. *Revista do Instituto de Medicina tropical de São Paulo* **6**, 93–100.

Cogo, J., Caleare, A. O., Ueda-Nakamura, T., Dias Filho, B. P., Ferreira, I. C. P. and Nakamura, C. V. (2012). Trypanocidal activity of guaianolide obtained from *Tanacetum parthenium* (L.) Schultz-Bip. and its combinational effect with benznidazole. *Phytomedicine* **1**, 59–66. doi: 10.1016/j.phymed.2012.09.011.

Dantas, A. P., Barbosa, H. S. and De Castro, S. L. (2003). Biological and ultrastructural effects of the anti-microtubule agent taxol against *Trypanosoma cruzi*. *Journal of Submicroscopic Cytology and Pathology* **35**, 287–294.

Fernandes, M. C., Da Silva, E. N., Jr., Pinto, A. V., De Castro, S. L. and Menna-Barreto, R. F. S. (2012). A novel triazolic naphthofuranqui-none induces autophagy in reservosomes and impairment of mitosis

in *Trypanosoma cruzi*. *Parasitology* **139**, 26–36. doi: 10.1017/S0031182011001612.

Gump, J. M. and Thorburn, A. (2011). Autophagy and apoptosis: what is the connection? *Trends in Cell Biology* **21**, 387–392. doi: 10.1016/j.tcb.2011.03.007.

Henriques, C., Moreira, T. L. B., Maia-Brigagão, C., Henriques-Pons, A., Carvalho, T. M. U. and De Souza, W. (2011). Tetrazolium salts based methods for high-throughput evaluation of anti-parasite chemotherapy. *Analytical Methods* **3**, 2148–2155.

Huber, K., Schemies, J., Uciechowska, U., Wagner, J. M., Rumpf, T., Lewrick, F., Süss, R., Sippl, W., Jung, M. and Bracher, F. (2010). Novel 3-arylideneindolin-2-ones as inhibitors of NAD$^+$-dependent histone deacetylases (sirtuins). *Journal of Medicinal Chemistry* **53**, 1383–1386. doi: 10.1021/jm901055u.

Kohl, L. and Bastin, P. (2003). The flagellum of trypanosomes. *International Review of Cytology* **244**, 227–285.

Kohl, L., Robinson, D. and Bastin, P. (2003). Novel roles for the flagellum in cell morphogenesis and cytokinesis of trypanosomes. *EMBO Journal* **22**, 5336–5346.

Lee, S. H., Meng, X. W., Flatten, K. S., Loegering, D. A. and Kaufmann, S. H. (2013). Phosphatidylserine exposure during apoptosis reflects bidirectional trafficking between plasma membrane and cytoplasm. *Cell Death and Differentiation* **20**, 64–76. doi: 10.1038/cdd.2012.93.

Macedo-Silva, S. T., Silva, T. L. A. O., Urbina, J. A., De Souza, W. and Rodrigues, J. C. F. (2011). Antiproliferative, ultrastructural, and physiological effects of amiodarone on promastigote and amastigote forms of *Leishmania amazonensis*. *Molecular Biology International* 876021. doi: 10.4061/2011/876021.

Meirelles, M. N., De Araújo Jorge, T. C. and De Souza, W. (1982). Interaction of *Trypanosoma cruzi* with macrophages *in vitro*: dissociation of the attachment and internalization phases by low temperature and cytochalasin B. *Zeitschrift für Parasitenkunde* **68**, 7–14.

Nakagawa, T. and Guarente, L. (2011). Sirtuins at a glance. *Journal of Cell Science* **124**, 833–838. doi: 10.1242/jcs.081067.

Religa, A. A. and Waters, A. P. (2012). Sirtuins of parasitic protozoa: in search of function(s). *Molecular and Biochemical Parasitology* **185**, 71–88. doi: 10.1016/j.molbiopara.2012.08.003.

Salminen, A. and Kaarniranta, K. (2009). SIRT1: regulation of longevity via autophagy. *Cellular Signalling* **21**, 1356–1360. doi: 10.1016/j.cellsig.2009.02.014.

Soeiro, M. N. C. and Castro, S. L. (2011). Screening of potential anti-*Trypanosoma cruzi* candidates: *in vitro* and *in vivo* studies. *Open Medicinal Chemistry Journal* **5**, 21–30. doi: 10.2174/1874104501105010021.

Silva, C. F., Daliry, A., Bernardino, P., Silva, P. B., Akay, S., Banerjee, B., Farahat, A. A., Fisher, M., Hu, L., Kumar, A., Liu, Z., Stephens, C. E., Boykin, D. and Soeiro, M. N. C. (2011). The efficacy of novel arylimidamides against *Trypanosoma cruzi in vitro*. *Parasitology* **138**, 1863–1869.

Tavares, J., Ouaissi, A., Kong Thoo Lin, P., Loureireo, I., Kaur, S., Roy, N. and Cordeiro-Da-Silva, A. (2010). Bisnaphthalimidopropyl derivatives as inhibitors of *Leishmania* SIR2 related protein 1. *ChemMedChem* **5**, 140–147.

Urbina, J. A. (2010). New insights in Chagas' disease treatment. *Drugs of the Future* **35**, 409–419. doi: 10.1358/dof.2010.35.5.1484391.

Veiga-Santos, P., Barrias, E. S., Santos, J. F. C., Moreira, T. L. B., Carvalho, T. M. U. and De Souza, W. (2012). Effects of amiodarone and posaconazole on the growth and ultrastructure of *Trypanosoma cruzi*. *International Journal of Antimicrobial Agents* **40**, 61–71. doi: 10.1016/j.ijantimicag.2012.03.009.

Verdin, E., Hirschey, M. D., Finley, L. W. S. and Haigis, M. C. (2010). Sirtuin regulation of mitochondria: energy production, apoptosis, and signaling. *Trends in Biochemical Sciences* **35**, 669–675. doi: 10.1016/j.tibs.2010.07.003.

Vergnes, B., Sereno, D., Madjidian-Sereno, N., Lemesre, J. L. and Ouaissi, A. (2002). Cytoplasmic SIR2 homologue overexpression promotes survival of *Leishmania* parasites by preventing programmed cell death. *Gene* **296**, 139–150. doi: 10.1016/S0378-1119(02)00842-9.

Vergnes, B., Vanhille, L., Ouaissi, A. and Sereno, D. (2005). Stage-specific antileishmanial activity of an inhibitor of SIR2 histone deacetylase. *Acta Tropica* **94**, 107–115. doi: 10.1016/j.actatropica.2005.03.004.

Voogd, T. E., Vansterkenburg, E. L. M., Wilting, J. and Janssen, L. H. M. (1993). Recent research on the biological activity of suramin. *Pharmacological Reviews* **46**, 177–199.

Zemzoumi, K., Sereno, D., Francois, C., Guilvard, E., Lemesre, J. L. and Ouaissi, A. (1998). *Leishmania major*: cell type dependent distribution of a 43 kDa antigen related to silent information regulatory-2 protein family. *Biology of the Cell* **90**, 239–245.

Zheng, W. (2013). Sirtuins as emerging anti-parasitic targets. *European Journal of Medicinal Chemistry* **59**, 132–140. doi: 10.1016/j.ejmech.2012. 11.014.

Zingales, B., Andrade, S. G., Briones, M. R. S., Campbell, D. A., Chiari, E., Fernandes, O., Guhl, F., Lages-Silva, E., Macedo, A. M., Machado, C. R., Miles, M. A., Romanha, A. J., Sturm, N. R., Tibayrenc, M. and Schijman, A. G. (2009). A new consensus for *Trypanosoma cruzi* intraspecific nomenclature: second revision meeting recommends TcI to TcVI. *Memórias do Instituto Oswaldo Cruz* **104**, 1051–1054.

World Health Organization (2013). *Control of Chagas Disease*. Fact sheet No 340 Updated March 2013. World Health Organization, Geneva, Switzerland.